Original Article | Neurointervention

eISSN 2005-8330
https://doi.org/10.3348/kjr.2021.0615
Korean J Radiol 2022;23(3):333-342

Korean Journal of Radiology
KJR

High-Resolution Intracranial Vessel Wall MRI Findings Among Different Middle Cerebral Artery Territory Infarction Types

So Yeon Won[1], Jihoon Cha[2], Hyun Seok Choi[3], Young Dae Kim[4], Hyo Suk Nam[4], Ji Hoe Heo[4], Seung-Koo Lee[2]

[1]Department of Radiology, Kangbuk Samsung Hospital, Sungkyunkwan University School of Medicine, Seoul, Korea; [2]Department of Radiology and Research Institute of Radiological Science, Severance Hospital, Yonsei University College of Medicine, Seoul, Korea; [3]Department of Radiology, Seoul Medical Center, Seoul, Korea; [4]Department of Neurology, Yonsei University College of Medicine, Seoul, Korea

Objective: Intracranial atherosclerotic stroke occurs through various mechanisms, mainly by artery-to-artery embolism (AA) or branch occlusive disease (BOD). This study evaluated the spatial relationship between middle cerebral artery (MCA) plaques and perforating arteries among different MCA territory infarction types using vessel wall magnetic resonance imaging (VW-MRI).

Materials and Methods: We retrospectively enrolled patients with acute MCA infarction who underwent VW-MRI. Thirty-four patients were divided into three groups according to infarction pattern: 1) BOD, 2) both BOD and AA (BOD-AA), and 3) AA. To determine the factors related to BOD, the BOD and BOD-AA groups were combined into one group (with striatocapsular infarction [BOD+]) and compared with the AA group. To determine the factors related to AA, the BOD-AA and AA groups were combined into another group (with cortical infarction [AA+]) and compared with the BOD group. Plaque morphology and the spatial relationship between the perforating artery orifice and plaque were evaluated both quantitatively and qualitatively.

Results: The plaque margin in the BOD+ group was closer to the perforating artery orifice than that in the AA group (p = 0.011), with less enhancing plaque (p = 0.030). In the BOD group, plaques were mainly located on the dorsal (41.2%) and superior (41.2%) sides where the perforating arteries mainly arose. No patient in the AA group had overlapping plaques with perforating arteries at the cross-section where the perforator arose. Perforating arteries associated with culprit plaques were most frequently located in the middle two-thirds of the M1 segment (41.4%). The AA+ group had more stenosis (%) than the BOD group (39.73 ± 24.52 vs. 14.42 ± 20.96; p = 0.003).

Conclusion: The spatial relationship between the perforating artery orifice and plaque varied among different types of MCA territory infarctions. In patients with BOD, the plaque margin was closer and blocked the perforating artery orifice, and stenosis degree and enhancement were less than those in patients with AA.

Keywords: *Artery-to-artery embolism; Atherosclerosis; Branch occlusive disease; Middle cerebral artery infarction; Vessel wall MRI*

INTRODUCTION

Intracranial atherosclerosis is one of the major causes of stroke, especially in the Asian population [1]. It can be caused by various mechanisms, mainly artery-to-artery embolism (AA) or branch occlusive disease (BOD) [2]. BOD is caused by occlusion of the perforating artery orifice by atherosclerotic plaque, which differs from AA [3]. Several previous studies compared high-resolution vessel wall magnetic resonance imaging (VW-MRI) characteristics between BOD and non-BOD patient groups. These studies showed that the BOD group differed in remodeling pattern,

Received: August 1, 2021 **Revised:** November 13, 2021 **Accepted:** December 9, 2021
Corresponding author: Jihoon Cha, MD, PhD, Department of Radiology and Research Institute of Radiological Science, Severance Hospital, Yonsei University College of Medicine, 50-1 Yonsei-ro, Seodaemun-gu, Seoul 03722, Korea.
• E-mail: jihooncha@yuhs.ac

stenosis degree, and plaque enhancement when compared to the non-BOD group (AA) [4,5], and that the BOD group had more frequent plaques on the superior or upper dorsal side of the middle cerebral artery (MCA) [4-8]. Although previous studies [4-8] have evaluated MCA plaque distribution in patients with BOD, only qualitative assessments were conducted by dividing the plaque distribution into two, four, or six sections. These previous studies have limitations in that they only evaluated the location of the plaque itself without considering the spatial relationship between the plaque and MCA perforating arteries. In addition, these studies determined MCA plaque location on sagittal images using absolute coordinates, although the location of the plaque or perforating arteries should be determined on a cross-section, perpendicular to the MCA course; this is because the MCA is not straight-shaped—it presents various shapes such as U-shape, inverted U-shape, and S-shape [6]. To overcome these limitations, the spatial relationship between MCA plaque and perforating arteries was evaluated in cross-sectional images perpendicular to the course of the MCA using a three-dimensional (3D) image, which has not been studied so far. To the best of our knowledge, quantitative evaluation of the spatial relationship between MCA plaques and perforating arteries has not been reported. In addition, the non-BOD group classified in the previous study [4] could be misclassified as it includes both BOD caused by atherosclerosis near the orifice of the perforating artery and artery-to-artery embolic infarction. Therefore, in our study, the group was classified separately in cases in which atherosclerosis was located in the orifice of the perforating artery, simultaneously resulting in both perforator infarction and cortical infarction due to distal embolization. Considering that plaque rupture is more prone to occur at the shoulder of the carotid plaque [9-12], we assumed that the distance between it and the perforating artery orifice may be closer in the BOD group. This study aimed to evaluate the spatial relationship between MCA plaque and perforating arteries among different types of MCA territory infarction using high-resolution VW-MRI.

MATERIALS AND METHODS

Patients

This retrospective study was approved by the Institutional Review Board of our institution (IRB No. 4-2020-0973). The requirement for informed patient consent was waived owing to the retrospective study design. A total of 380 patients underwent VW-MRI between April 2017 and October 2019 at our institution. We included patients with a history of acute MCA infarction confirmed by DWI within 1 month (n = 48). Two neuroradiologists independently reviewed the images (with 10 and 2 years of experience in neuroradiology, respectively). If disagreements occurred between the reviewers, a final decision was made through consensus. Patients with a potential source of cardioembolism, extracranial atherosclerosis with significant stenosis, other stroke etiology (moyamoya disease [n = 4], dissection [n = 4]), or poor-quality images (n = 6) were excluded. The final 34 patients were divided into three groups according to the infarction pattern (Fig. 1): 1) BOD, patients with striatocapsular infarction only (n = 17), 2) BOD-AA (both BOD and AA), patients with simultaneous MCA infarction in the cortical/subcortical and striatocapsular area (n = 9), and 3) AA group, patients with MCA territory infarction without infarction in the striatocapsular area (n = 8). To overcome the overlapping part of the BOD-AA group, a subgroup analysis was performed. For subgroup analysis, BOD and BOD-AA groups were combined into one group (with striatocapsular infarction [BOD+], n = 26) and compared with the AA group (without striatocapsular infarction) to identify the factors related to BOD. The BOD-AA and AA groups were combined into another group (with cortical infarction [AA+], n = 17) and then compared with the BOD group (without cortical infarction) to identify the factors related to AA.

MRI Review

The imaging parameters are described in Supplement. All analyses were performed on cross-sectional images perpendicular to the course of the MCA acquired using a 3D Slicer (3D Slicer v4.10.2) [13]. Plaque and perforating arteries were identified on the PD sequence, which provides sharp delineation of the arterial walls between flowing blood and cerebrospinal fluid with a high signal-to-noise ratio. Plaque enhancement was evaluated using a 3D fat-suppressed post-contrast T1-weighted image. Vessel lumens were identified using a 3D fat-suppressed T1-weighted image. For quantitative analysis, post-contrast T1-weighted and T1-weighted images were co-registered to PD images using rigid body transformation.

Spatial Relationship between the Perforating Arteries and Plaque

To evaluate the spatial relationship between the

https://doi.org/10.3348/kjr.2021.0615

Korean Journal of Radiology
KJR

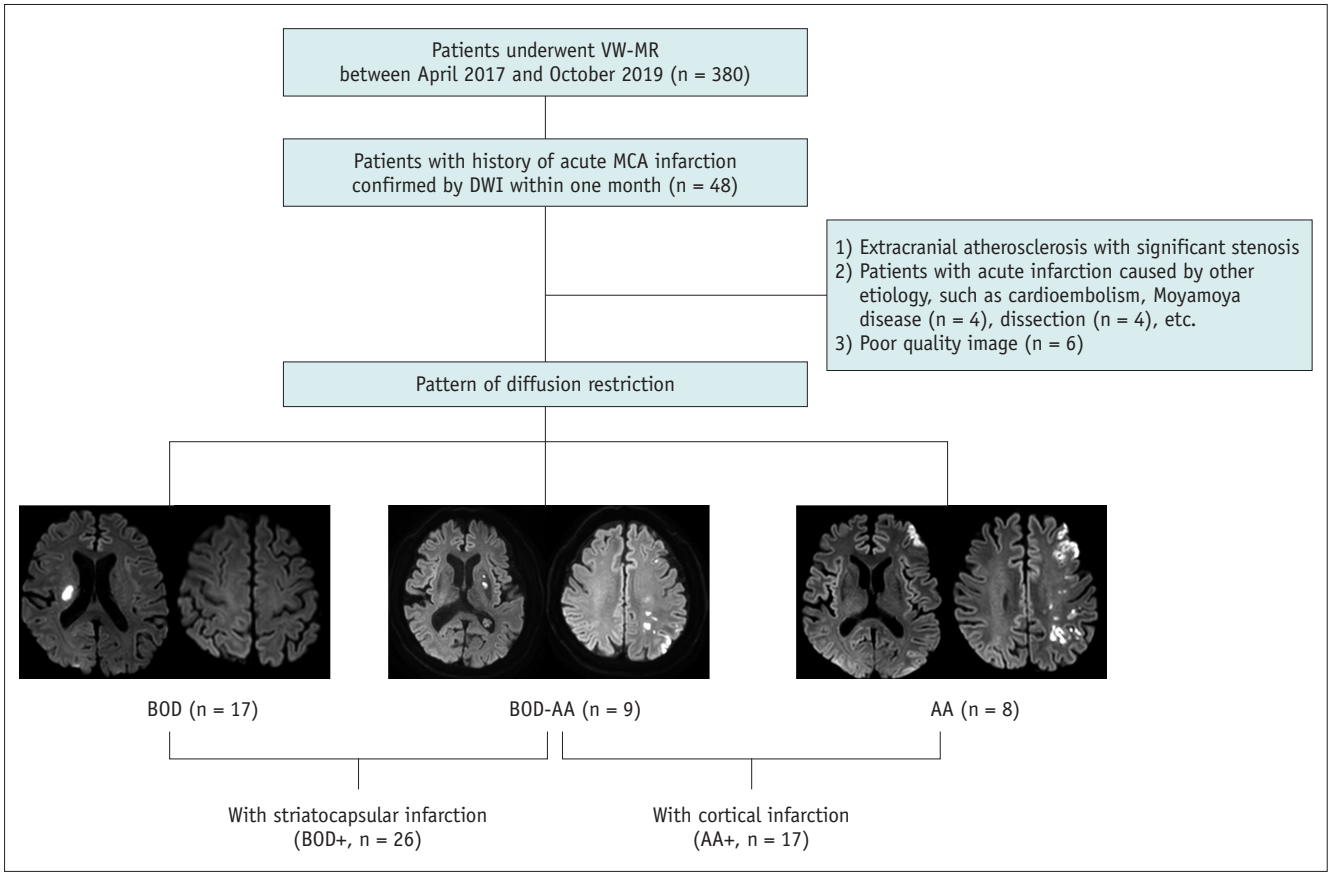

Fig. 1. Diagram of patient selection. AA = artery-to-artery embolism, BOD = branch occlusive disease, DWI = diffusion weighted imaging, MCA = middle cerebral artery, VW = vessel wall

perforating arteries and plaque, cross-sectional images perpendicular to the MCA course in which the perforator arose were selected. The location of both the perforating arteries arising from the M1 portion of the MCA and the margin of the plaque were described in angle (°) on the PD sequence using the following angular location definitions, 0°, 90°, 180°, and 270° for the ventral, superior, dorsal, and inferior sides, respectively. Similarly, plaque distribution was expressed as the angle range of the PD sequence. In addition, the longitudinal location of the perforating artery and the most stenotic portion were also calculated as a ratio—distance from the internal carotid artery (ICA) to the perforator or the most stenotic portion/length of the M1 segment (distance from the ICA to the terminal of the M1 segment). The location of the perforating artery or plaque was also qualitatively evaluated by dividing it into four sections (ventral, superior, dorsal, and inferior). Plaque blockage of the perforator orifice was compared between the groups. To evaluate the proximity of the perforating artery orifice to the plaque margin, the angular difference between them was calculated and compared among the groups.

Morphological Characteristics of MCA

The outer wall and lumen were manually drawn in cross-sectional images on T1-weighted images with reference to the co-registered PD images at three locations: 1) perforator origin, 2) the most stenotic MCA portion, and 3) normal reference vessel (contralateral or proximal to the stenotic portion). The region of interests were first drawn by a junior neuroradiologist and then confirmed by a senior neuroradiologist with 9 years of experience. The wall area was calculated by subtracting the lumen area from the outer wall area. Stenosis degree was calculated as follows: (1-lumen area/reference lumen area) x 100%; the remodeling index was calculated as follows: outer wall area/reference outer wall area. The region of interest of enhancing plaque was drawn in a slice section with the largest portion of enhancing plaque. The enhancement ratio was calculated as follows: (signal intensity of post-contrast T1-wighted image – signal intensity of T1-weighted image)/ signal intensity of T1-weighted image. The 95th percentiles

https://doi.org/10.3348/kjr.2021.0615

of the enhancement ratios were recorded.

Statistical Analyses

The Shapiro-Wilk test for normality and Levene's F test for equal variance were performed for continuous data. To compare features among groups, the Mann-Whitney U test or Kruskal-Wallis test was used for data without normality and equal variance. Student's *t* test or analysis of variance was used for continuous data with normality and equal variance. For categorical variables, the chi-square test or Fisher's exact test was used. Data are presented as the mean ± standard deviation. All statistical analyses were performed with SPSS (version 25.0; IBM Corp.) and R statistical software v.3.6.1 (R Foundation for Statistical Computing).

RESULTS

Thirty-four patients were included (male, n = 21 [61.8%]; age, 58.2 ± 14.4 years). Seventeen patients (50.0%) were included in the BOD, nine patients (26.5%) in the BOD-AA, and eight patients (23.5%) in the AA group. Representative cases are shown in Figures 2 and 3. The clinical characteristics of the three groups were compared (Supplementary Table 1).

Spatial Relationship between the Perforating Artery Orifice and Plaque

The proportion of patients whose perforator orifice was blocked by plaque significantly differed among the groups (BOD vs. BOD-AA vs. AA, $p < 0.001$) (Table 1). In the post-hoc analysis, BOD (94.1%) and BOD-AA (88.9%) groups had a higher proportion of patients with a plaque-blocked perforator orifice than the AA group (0.0%) ($p < 0.001$ and $p < 0.001$, respectively). There were no cases of such blockage in the AA group.

The proximity of the perforating artery orifice to the plaque margin was considered close if the angular difference between them was < 15°. There was a significant difference in the proportion of patients with a close orifice and plaque

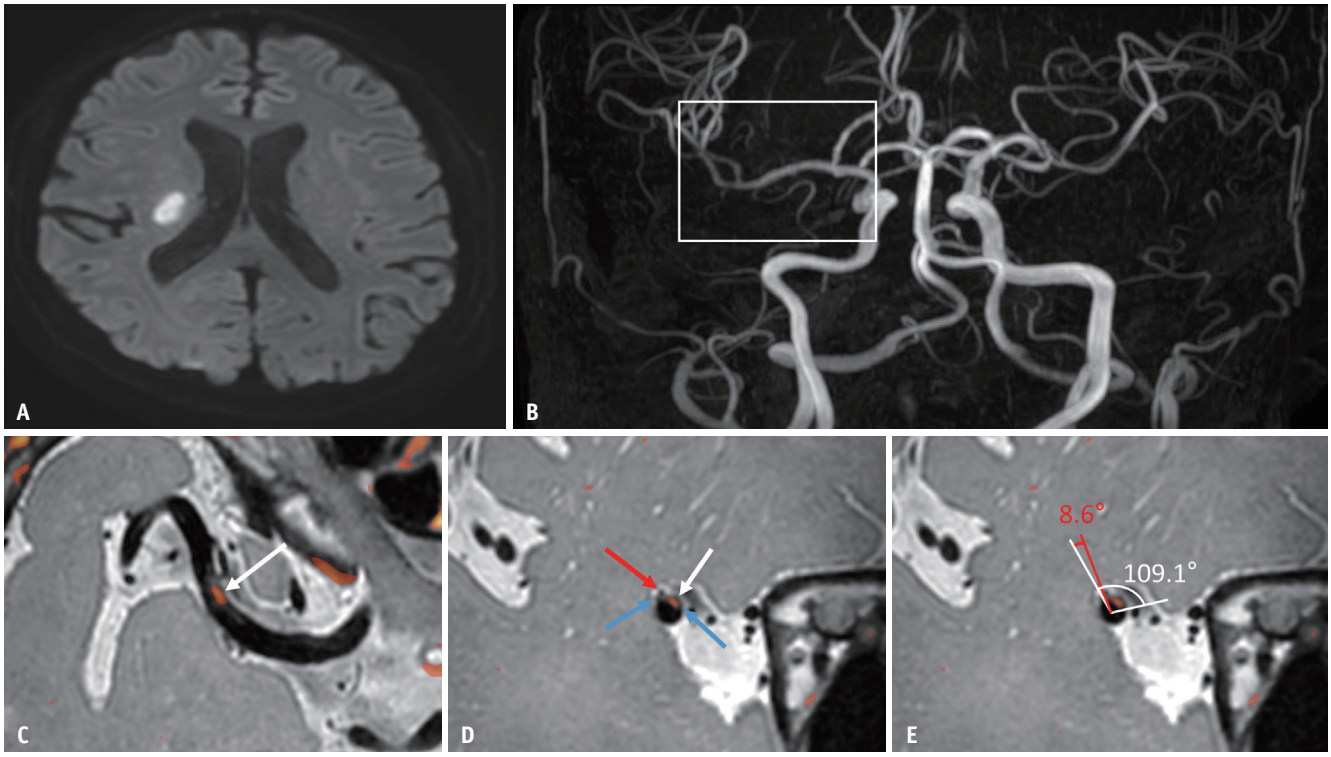

Fig. 2. Representative case with BOD.
A. Acute infarction in the right striatocapsular territory on a diffusion-weighted image. **B.** No significant stenosis of the right MCA M1 segment is noted on TOF MR angiography. **C.** Curved planar reformation of fusion image (PD + post-contrast T1-weighted image) in the white box on **(B)**. The plaque enhancement on post-contrast T1-weighted image is expressed as a color map (orange color, arrow). **D.** Perpendicular image where the perforator arouse. Perforator (red arrow), plaque (white arrow), and margin of the plaque (blue arrows). **E.** Plaque distribution is expressed as an angle (white line) on the PD image. Angular difference is expressed as an angle between the white and red lines. Perforator is shown to originate at the margin of the plaque. BOD = branch occlusive disease, MCA = middle cerebral artery, PD = proton density imaging, TOF = time of flight

https://doi.org/10.3348/kjr.2021.0615

Korean Journal of Radiology
KJR

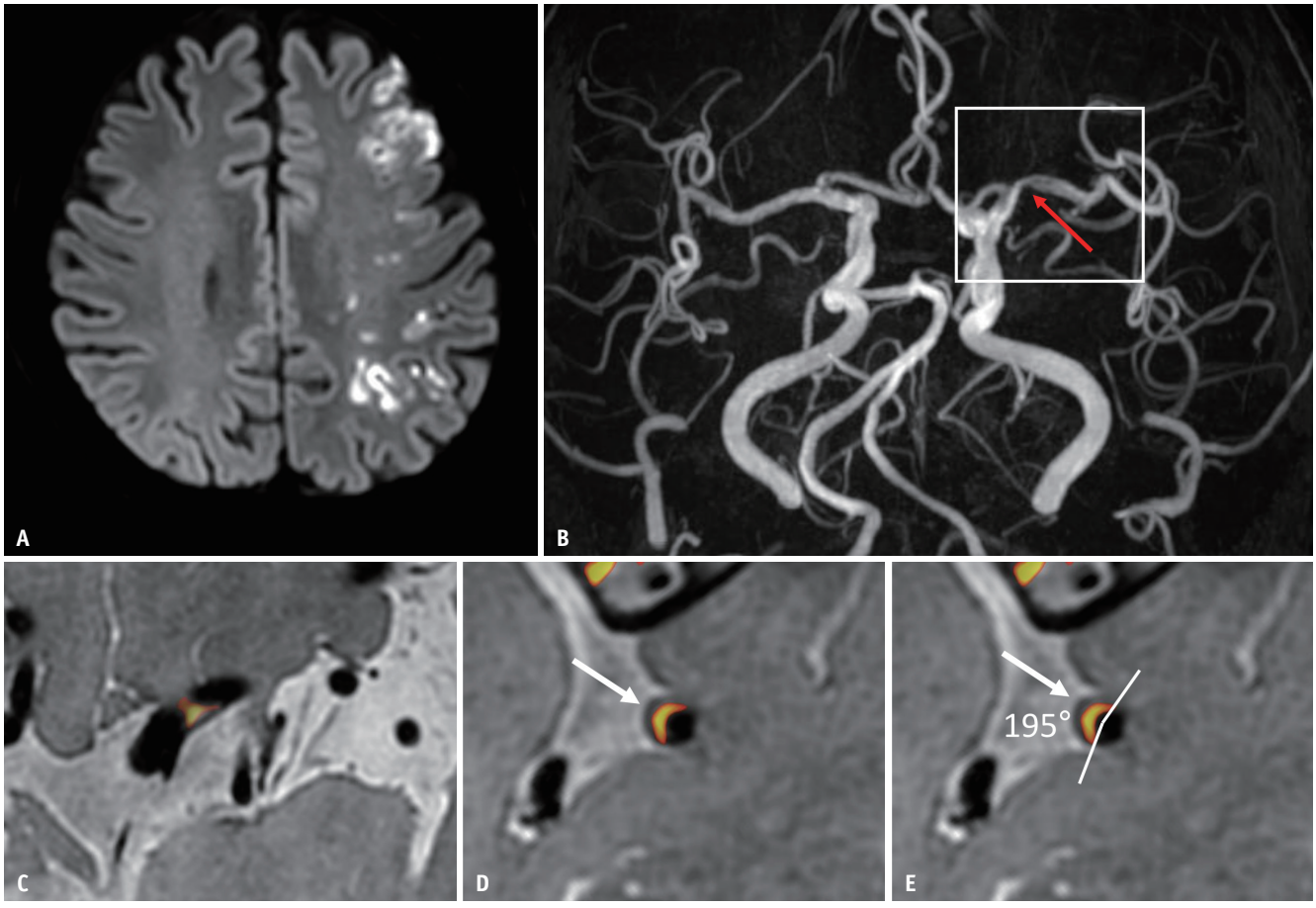

Fig. 3. Representative case with AA.
A. Acute infarction in the left MCA territory on a diffusion-weighted image. **B.** Significant focal stenosis is seen in the M1 segment of MCA on TOF MR angiography (arrow). **C.** Curved planar reformation of fusion image (PD + post-contrast T1-weighted image) in the white box on **(B)**. The plaque enhancement on post-contrast T1-weighted image is expressed by a color map (orange color). **D.** Perpendicular image of the plaque (arrow). **E.** Plaque (arrow) distribution is expressed as an angle. In this case, the perforator does not originate near the plaque. AA = artery-to-artery embolism, MCA = middle cerebral artery, PD = proton density imaging, TOF = time of flight

Table 1. Qualitative and Quantitative Comparison of the Spatial Relationship between Orifice of the Perforator and Plaque

	Orifice of Perforator Blocked by the Plaque		*P*	Angular Difference < 15°		*P*	Angular Range of Plaque (Mean Degree ± SD)	*P*
	No	Yes		No	Yes			
Comparison among three groups			< 0.001			0.019		0.106
BOD (n = 17)	1 (5.9)	16 (94.1)		5 (29.4)	12 (70.6)		122.3° ± 79.4°	
BOD-AA (n = 9)	1 (11.1)	8 (88.9)		3 (33.3)	6 (66.7)		189.2° ± 55.4°	
AA (n = 8)	8 (100.0)	0 (0.0)		7 (87.5)	1 (12.5)		151.4° ± 51.6°	
Comparison between BOD and AA+			0.003			0.084		0.051
BOD (n = 17)	1 (5.9)	16 (94.1)		5 (29.4)	12 (70.6)		122.3° ± 79.4°	
AA+ (n = 17)	9 (52.9)	8 (47.1)		10 (58.8)	7 (41.2)		176.6° ± 55.0°	
Comparison between AA and BOD+			< 0.001			0.011		0.851
AA (n = 8)	8 (100.0)	0 (0.0)		7 (87.5)	1 (12.5)		151.4° ± 51.6°	
BOD+ (n = 26)	2 (7.7)	24 (92.3)		8 (30.8)	18 (69.2)		143.7° ± 78.2°	

Data are number of patients with % in parentheses unless specified otherwise. Chi-square or Fisher exact test was performed. Spatial relationship was measured at the cross-sectional image perpendicular to middle cerebral artery course in which perforator arising. BOD-AA group and AA group were combined as AA+ group. BOD group and BOD-AA group were combined as BOD+ group. *p* value was corrected by Bonferroni correction. AA = artery-to-artery embolism, BOD = branch occlusive disease, SD = standard deviation

https://doi.org/10.3348/kjr.2021.0615

margin among the groups (BOD vs. BOD-AA vs. AA, p = 0.019, Table 1). In the post-hoc analysis, the BOD (70.6%) group had a higher proportion of patients with an angular difference < 15° than the AA group (12.5%; p = 0.033). The angular plaque range in the BOD-AA group (189.2° ± 55.4°) was significantly larger than that in the BOD group (122.3° ± 79.4°, p = 0.043).

In the subgroup analysis, the BOD+ group had a significantly higher proportion of patients with a plaque-blocked orifice than the AA group (92.3% vs. 0.0%; p < 0.001). The BOD+ group had a higher proportion of patients (69.2%) with a close perforating artery orifice and plaque margin than the AA group (12.5%; p = 0.011). The AA+ group tended to have a larger angular plaque range than the BOD group on cross-sectional images perpendicular to the MCA course in which the perforator arose (176.6° ± 55.0° vs. 122.3° ± 79.4°, p = 0.051).

Perforating Artery Orifice and Plaque Distributions

Perforating artery orifices were located in the dorsal (47.1%), superior (44.1%), and inferior (8.8%) walls of the cross-sectional images (Table 2). The perforating arteries mainly arose in the dorsal and superior walls of the MCA. The location of the perforating artery orifice, according to the four cross-sectional portions, did not significantly differ among the groups (p = 0.256).

The plaque location in the cross-sectional images in which the perforator arose significantly differed among the groups (p = 0.002). In the post-hoc analysis, there was a significant difference between BOD and BOD-AA groups (p = 0.014), between the BOD and AA groups (p = 0.032), and between the BOD-AA and AA groups (p = 0.027). In the BOD group, plaque centers were mainly located in the dorsal (41.2%) and superior (41.2%) walls in which the perforators mainly arose. In the BOD-AA groups, plaques were most commonly located in the ventral wall (55.6%), followed by the superior wall (22.2%). In the AA groups, plaque was absent in the cross-sections in which the perforators arose in half of the cases. Even in cases with observable plaque in the cross-sectional images where the perforator arose, the plaque location and perforating artery orifice did not overlap.

In the most stenotic MCA cross-sections, plaques were commonly located in the order of superior (35.3%), ventral (26.5%), inferior (20.6%), and dorsal (17.6%) walls. The plaque location according to the four portions in the most stenotic cross-sections did not significantly differ among

Table 2. Comparison of the Locations of Middle Cerebral Artery Perforator and Plaque according to 4-Sections

	Location of Orifice of Perforator			p	Blocked Perforator				p	Location of Plaque (Perforator Origin Site)					p	Location of Plaque (Most Stenotic Portion)				p
	Dorsal	Superior	Inferior		Dorsal	Superior	Inferior	Total		Dorsal	Superior	Ventral	Inferior	N/A		Dorsal	Superior	Ventral	Inferior	
Comparison among three groups				0.256					0.001						0.002					0.335
BOD (n = 17)	5 (29.4)	10 (58.8)	2 (11.8)		4/5 (80.0)	10/10 (100)	2/2 (100)	16/17 (94.1)		7 (41.2)	7 (41.2)	2 (11.8)	1 (5.9)	0 (0.0)		3 (17.6)	9 (52.9)	3 (17.6)	2 (11.8)	
BOD-AA (n = 9)	6 (66.7)	3 (33.3)	0 (0.0)		5/6 (83.3)	3/3 (100)	0/0 (0.0)	8/9 (88.9)		0 (0.0)	2 (22.2)	5 (55.6)	1 (11.1)	1 (11.1)		2 (22.2)	1 (11.1)	4 (44.4)	2 (22.2)	
AA (n = 8)	5 (62.5)	2 (25.0)	1 (12.5)		0/5 (0.0)	0/2 (0.0)	0/1 (0.0)	0/8 (0.0)		2 (25.0)	2 (25.0)	0 (0.0)	0 (0.0)	4 (50.0)		1 (12.5)	2 (25.0)	2 (25.0)	3 (37.5)	
Comparison between BOD and AA+				0.123					0.003						0.029					0.148
BOD (n = 17)	5 (29.4)	10 (58.8)	2 (11.8)		4/5 (80.0)	10/10 (100)	2/2 (100)	16.17 (94.1)		7 (41.2)	7 (41.2)	2 (11.8)	1 (5.9)	0 (0.0)		3 (17.6)	9 (52.9)	3 (17.6)	2 (11.8)	
AA+ (n = 17)	11 (64.7)	5 (29.4)	1 (5.9)		5/11 (45.5)	3/5 (60.0)	0/1 (0.0)	8/17 (47.1)		2 (11.8)	4 (23.5)	5 (29.4)	1 (5.9)	5 (29.4)		3 (17.6)	3 (17.6)	6 (35.3)	5 (29.4)	
Comparison between AA and BOD+				0.398					< 0.001						0.026					0.638
AA (n = 8)	5 (62.5)	2 (25.0)	1 (12.5)		0/5 (0.0)	0/2 (0.0)	0/1 (0.0)	0/8 (0.0)		2 (25.0)	2 (20.0)	0 (0.0)	0 (0.0)	4 (50.0)		1 (12.5)	2 (25.0)	2 (25.0)	3 (37.5)	
BOD+ (n = 26)	11 (42.3)	13 (50.0)	2 (7.7)		9/11 (81.8)	13/13 (100)	2/2 (100)	24/26 (92.3)		7 (26.9)	9 (34.6)	7 (26.9)	2 (7.7)	1 (3.8)		5 (19.2)	10 (38.5)	7 (26.9)	4 (15.4)	

Data are number of patients with % in parentheses. BOD-AA group and AA group were combined as AA+ group. BOD group and BOD-AA group were combined as BOD+ group. p value was corrected by Bonferroni correction. AA = artery-to-artery embolism, BOD = branch occlusive disease

https://doi.org/10.3348/kjr.2021.0615

Korean Journal of Radiology
KJR

the groups (p = 0.335).

The longitudinal location of the perforating artery (ratio of the distance from the ICA to perforator/distance from the ICA to the terminal of the M1 segment) was 0.46 (interquartile range: 0.31–0.71) (Supplementary Table 2). Perforating arteries associated with culprit plaques were the most frequently located in the middle two-thirds of the M1 segment (41.4%). There was no significant difference in the location of the perforating artery among the groups (median [interquartile range]: 0.48 [0.36–0.75], 0.36 [0.20–0.70], and 0.32 [0.29–0.62], respectively; p = 0.205).

The longitudinal location of the most stenotic portion (ratio of distance from ICA to most stenotic portion/ distance from ICA to terminal of M1 segment) was 0.47 (interquartile range: 0.19–0.78). Seventeen (50%) of 34 patients had proximal stenosis. There was no significant difference in the location of the most stenotic portion among BOD, BOD-AA, and AA (0.47 [0.30–0.77], 0.29 [0.14–0.74], and 0.59 [0.14–0.93], respectively; p = 0.540).

Plaque Morphological Characteristics

The BOD group had distinct radiologic findings in terms of plaque enhancement and plaque morphology (Table 3). The plaque extent (mm) in the longitudinal plane significantly differed among the BOD, BOD-AA, and AA groups (6.82 ± 3.49, 10.83 ± 5.44, and 11.56 ± 4.87, respectively; p = 0.026). There was a significant difference in stenosis degree (%) in the most stenotic portion among the BOD, BOD-AA, and AA groups (14.42% ± 20.96%, 41.79% ± 25.33%, and 37.42% ± 25.09%, respectively; p = 0.012).

In subgroup analysis, the plaque extent in the longitudinal plane was significantly larger in the AA+ groups than in the BOD groups (11.18 ± 5.16 vs. 6.82 ± 3.49; p = 0.007).

The AA+ group had more stenosis (%) than the BOD group (39.73 ± 24.52 vs. 14.42 ± 20.96%; p = 0.003).

DISCUSSION

We utilized VW-MRI to evaluate the spatial relationship between MCA plaque and perforating arteries among different types of MCA territory infarctions. To compare the two groups from two perspectives (the factors related to BOD or AA), both the BOD and BOD-AA groups were combined into the BOD+ group, and the BOD-AA and AA groups were combined into the AA+ group.

The BOD+ (BOD and BOD-AA) group had a plaque

Table 3. Comparison of Morphological Characteristics of MCA

	Enhancement Ratio (95 Percentile)	*P*	Maximum Extent of Largest Plaque (mm)	*P*	Stenosis Degree (%) at Perforator Arise*	*P*	Stenosis Degree (%) at Most Stenotic†	*P*	Remodeling Index at Perforator Arise*	*P*	Remodeling Index at Most Stenotic†	*P*
Comparison among three groups		0.070		0.026		0.309		0.012		0.364		0.837
BOD (n = 17)	1.6 ± 0.9		6.8 ± 3.5		8.3 ± 21.5		14.4 ± 21.0		1.1 ± 0.1		1.0 ± 0.14	
BOD-AA (n = 9)	2.4 ± 1.5		10.8 ± 5.4		23.9 ± 34.4		41.8 ± 25.3		0.9 ± 0.3		1.0 ± 0.12	
AA (n = 8)	2.6 ± 0.6		11.6 ± 5.2		7.0 ± 26.1		37.4 ± 25.1		0.9 ± 0.4		1.0 ± 0.13	
Comparison between BOD and AA+		0.023		0.007		0.411		0.003		0.159		0.990
BOD (n = 17)	1.6 ± 0.9		6.8 ± 3.5		8.3 ± 21.5		14.4 ± 21.0		1.1 ± 0.1		1.0 ± 0.14	
AA+ (n = 17)	2.5 ± 1.1		11.2 ± 5.2		16.0 ± 31.1		39.7 ± 24.5		0.9 ± 0.3		1.0 ± 0.13	
Comparison between AA and BOD+		0.030		0.089		0.542		0.201		0.583		0.612
AA (n = 8)	2.6 ± 0.6		11.6 ± 5.2		7.0 ± 26.1		37.4 ± 25.1		0.9 ± 0.4		1.0 ± 0.13	
BOD+ (n = 26)	1.9 ± 1.2		8.2 ± 4.6		13.7 ± 27.1		23.9 ± 25.7		1.0 ± 0.2		1.0 ± 0.13	

Values are presented as mean ± standard deviation. BOD-AA group and AA group were combined as AA+ group. BOD group and BOD-AA group were combined as BOD+ group. p value was corrected by Bonferroni correction. *Calculated at the cross-sectional images in which perforators arise, †Calculated at the cross-sectional images with most stenotic portion of MCA. AA = artery-to-artery embolism, BOD = branch occlusive disease, MCA = middle cerebral artery

https://doi.org/10.3348/kjr.2021.0615

margin closer to the perforating artery orifice and had a significantly higher proportion of a plaque-blocked orifice than the AA group. The perforator orifices were mainly located on the dorsal and superior walls of the MCA. The plaque location at the cross-section in which the perforator arose differed significantly between the groups. No patient in the AA group had plaque or overlapping plaque with perforators at the cross-section where the perforator arose. The perforating artery associated with the culprit plaque was the most frequently located in the middle two-thirds of the M1 segment. The plaque extent in both the longitudinal and cross-sectional planes perpendicular to the MCA course was significantly larger in the AA+ group (AA and BOD-AA) than in the BOD group. Patients in the BOD group had less stenosis and enhancement than those in the AA+ group.

While none of the patients with AA had perforator orifices blocked by plaque, the majority of patients in the BOD and BOD-AA groups did. This finding is consistent with the mechanism of BOD caused by perforating artery orifice blockage by atherosclerosis. In a previous study [4] that compared BOD and non-BOD groups, the non-BOD group was defined as patients with infarction beyond the striatocapsular area. However, in our study, the AA+—defined as a non-BOD group as that in the previous study—was further divided into the BOD-AA and AA groups and then compared. Most patients with BOD-AA had plaque-blocked perforating artery orifices. Given these differences, these two groups may need to be considered separately.

Plaque rupture is more prone to occur in the shoulder of the carotid plaque [9-12]. The maximum circumferential stress appears at the plaque shoulder [9] and activated metalloproteinase may often be expressed in the shoulder of vulnerable plaque [14-16]. Our results showed that the BOD+ group had a higher proportion of patients with close perforator orifices and plaque margins than those in the AA group, thereby supporting our assumption.

In our study, the perforating artery orifices were mainly located on the dorsal and superior walls of the MCA, regardless of the group, consistent with the results of previous studies [17,18]. Other studies have shown that superior wall plaque located near the perforating artery orifice causes more symptoms by blocking the orifice [8,19], and that many patients with BOD have plaques on the upper dorsal side [7]. However, a previous study [20] showed that plaque location did not significantly differ between patients with BOD and those with small vessel occlusive disease. This is probably due to the evaluation being based on the plaque center; it is important to evaluate the relationship with the perforating artery by considering the plaque margin.

Therefore, in our study, the proximity of the plaque margin and perforating artery orifice was evaluated in both the short- and long-axis views. The majority of patients in the BOD group had plaques located on the superior or dorsal wall where the perforators mainly arose. However, the plaque was mainly located on the ventral wall of the MCA in BOD-AA group. This difference could be due to the limitation in the process of classifying the plaque location in the short-axis view. In fact, the plaque location is not limited to one quadrant, but can be distributed across several quadrants of the MCA wall if the angular range of the plaque is wide. We posited that the ventrally located plaque in the BOD-AA was sufficient to be extended to the margin of the perforator. The plaque range in the BOD-AA group was significantly higher than that in the BOD group. Additionally, eight of the nine patients with BOD-AA showed plaque blockage (Table 1). These results support this assumption.

In most MCA plaque distribution studies, only the short-axis view (e.g., superior, inferior, dorsal, and ventral) was evaluated. In our study, the location of the perforating artery and stenosis were also evaluated by dividing them into proximal, middle, and distal portions, and the distribution was evaluated as the ratio of the total length of the MCA M1 segment. The perforating artery associated with the culprit plaque was most frequently located in the middle segment of M1, and stenosis most frequently occurred in the proximal third segment of M1. Since the perforating arteries are mainly located in the middle segment and superior/dorsal surface of M1, BOD will occur when plaques form in this location. Atherosclerotic plaques occur mainly in areas with low wall shear stress [21,22]. As plaques protrude into the lumen, an area with high wall shear stress is formed, where the risk of plaque rupture is high [23]. To determine why plaque occurs in the superior/dorsal wall of the middle portion of the MCA in patients with BOD, further research on MCA geometry and hemodynamics is needed.

The AA+ group had more stenosis cases than the BOD group, which is consistent with previous studies [4,24]. The degree of plaque enhancement was higher in the AA+ group than in the BOD group, which is consistent with previous studies [4,25]. The stenosis degree in the AA+ group was higher than that in the BOD group, consistent with previous findings [4,5].

https://doi.org/10.3348/kjr.2021.0615

Korean Journal of Radiology
KJR

VW-MRI findings can help evaluate stroke etiology and determine the treatment plan by distinguishing BOD and AA through the proximity of the plaque margin and perforating artery orifice, even if MCA stenosis is not significant on MR angiography. However, in such cases, nonstenotic culprit plaques can be missed, and the stroke etiology can be misclassified as embolic infarction or small vessel disease without VW-MRI. This can also affect the treatment plan.

This study has some limitations. First, the sample size was small, and patients from only a single center were included. Second, we only included patients with acute MCA infarction confirmed by DWI within 1 month to evaluate VW-MRI findings in the acute stage. Hence, further studies with larger sample sizes should be performed to validate our findings. Lastly, atherosclerosis was not pathologically confirmed.

In conclusion, the relationship between plaque and perforating arteries and that between plaque location and characteristics varied among different types of MCA territory infarction, as assessed using high-resolution VW-MRI. In patients with BOD, plaque margins were closer and blocked the perforating artery orifices and the stenosis degree and plaque enhancement were lesser than that in patients with AA.

Supplement

The Supplement is available with this article at https://doi.org/10.3348/kjr.2021.0615.

Availability of Data and Material

The datasets generated or analyzed during the study are available from the corresponding author on reasonable request.

Conflicts of Interest

The authors have no potential conflicts of interest to disclose.

Author Contributions

Conceptualization: Jihoon Cha. Data curation: So Yeon Won. Formal analysis: So Yeon Won. Investigation: So Yeon Won, Jihoon Cha. Methodology: Jihoon Cha. Project administration: Jihoon Cha. Resources: Hyun Seok Choi, Young Dae Kim, Hyo Suk Nam, Ji Hoe Heo. Software: Jihoon Cha. Supervision: Seung-Koo Lee. Validation: So Yeon Won, Jihoon Cha. Visualization: So Yeon Won, Jihoon Cha. Writing—original draft: So Yeon Won, Jihoon Cha. Writing—review & editing: Jihoon Cha, Hyun Seok Choi, Young Dae Kim, Hyo Suk Nam, Ji Hoe Heo.

ORCID iDs

So Yeon Won
https://orcid.org/0000-0003-0570-3365
Jihoon Cha
https://orcid.org/0000-0002-1662-8041
Hyun Seok Choi
https://orcid.org/0000-0003-4999-8513
Young Dae Kim
https://orcid.org/0000-0001-5750-2616
Hyo Suk Nam
https://orcid.org/0000-0002-4415-3995
Ji Hoe Heo
https://orcid.org/0000-0001-9898-3321
Seung-Koo Lee
https://orcid.org/0000-0001-5646-4072

Funding Statement

None

REFERENCES

1. Gorelick PB, Wong KS, Bae HJ, Pandey DK. Large artery intracranial occlusive disease: a large worldwide burden but a relatively neglected frontier. *Stroke* 2008;39:2396-2399
2. Shin DH, Lee PH, Bang OY. Mechanisms of recurrence in subtypes of ischemic stroke: a hospital-based follow-up study. *Arch Neurol* 2005;62:1232-1237
3. Caplan LR. Intracranial branch atheromatous disease: a neglected, understudied, and underused concept. *Neurology* 1989;39:1246-1250
4. Ryoo S, Lee MJ, Cha J, Jeon P, Bang OY. Differential vascular pathophysiologic types of intracranial atherosclerotic stroke: a high-resolution wall magnetic resonance imaging study. *Stroke* 2015;46:2815-2821
5. Ryoo S, Park JH, Kim SJ, Kim GM, Chung CS, Lee KH, et al. Branch occlusive disease: clinical and magnetic resonance angiography findings. *Neurology* 2012;78:888-896
6. Kim BJ, Yoon Y, Lee DH, Kang DW, Kwon SU, Kim JS. The shape of middle cerebral artery and plaque location: high-resolution MRI finding. *Int J Stroke* 2015;10:856-860
7. Sun LL, Li ZH, Tang WX, Liu L, Chang FY, Zhang XB, et al. High resolution magnetic resonance imaging in pathogenesis diagnosis of single lenticulostriate infarction with nonstenotic middle cerebral artery, a retrospective study. *BMC Neurol* 2018;18:51
8. Xu WH, Li ML, Gao S, Ni J, Zhou LX, Yao M, et al. Plaque

distribution of stenotic middle cerebral artery and its clinical relevance. *Stroke* 2011;42:2957-2959
9. Richardson PD, Davies MJ, Born GV. Influence of plaque configuration and stress distribution on fissuring of coronary atherosclerotic plaques. *Lancet* 1989;334:941-944
10. Shindo S, Fujii K, Shirakawa M, Uchida K, Enomoto Y, Iwama T, et al. Morphologic features of carotid plaque rupture assessed by optical coherence tomography. *AJNR Am J Neuroradiol* 2015;36:2140-2146
11. Thrysøe SA, Oikawa M, Yuan C, Eldrup N, Klaerke A, Paaske WP, et al. Longitudinal distribution of mechanical stresses in carotid plaques of symptomatic patients. *Stroke* 2010;41:1041-1043
12. Toutouzas K, Karanasos A, Tsiamis E, Riga M, Drakopoulou M, Synetos A, et al. New insights by optical coherence tomography into the differences and similarities of culprit ruptured plaque morphology in non-ST-elevation myocardial infarction and ST-elevation myocardial infarction. *Am Heart J* 2011;161:1192-1199
13. Fedorov A, Beichel R, Kalpathy-Cramer J, Finet J, Fillion-Robin JC, Pujol S, et al. 3D Slicer as an image computing platform for the quantitative imaging network. *Magn Reson Imaging* 2012;30:1323-1341
14. Brown DL, Hibbs MS, Kearney M, Loushin C, Isner JM. Identification of 92-kD gelatinase in human coronary atherosclerotic lesions. Association of active enzyme synthesis with unstable angina. *Circulation* 1995;91:2125-2131
15. de Kleijn DP, Sluijter JP, Smit J, Velema E, Richard W, Schoneveld AH, et al. Furin and membrane type-1 metalloproteinase mRNA levels and activation of metalloproteinase-2 are associated with arterial remodeling. *FEBS Lett* 2001;501:37-41
16. Tang D, Teng Z, Canton G, Yang C, Ferguson M, Huang X, et al. Sites of rupture in human atherosclerotic carotid plaques are associated with high structural stresses: an in vivo MRI-based 3D fluid-structure interaction study. *Stroke* 2009;40:3258-3263
17. Umansky F, Gomes FB, Dujovny M, Diaz FG, Ausman JI, Mirchandani HG, et al. The perforating branches of the middle cerebral artery. A microanatomical study. *J Neurosurg* 1985;62:261-268
18. Marinkovic SV, Milisavljevic MM, Kovacevic MS, Stevic ZD. Perforating branches of the middle cerebral artery. Microanatomy and clinical significance of their intracerebral segments. *Stroke* 1985;16:1022-1029
19. Yoon Y, Lee DH, Kang DW, Kwon SU, Kim JS. Single subcortical infarction and atherosclerotic plaques in the middle cerebral artery: high-resolution magnetic resonance imaging findings. *Stroke* 2013;44:2462-2467
20. Bae YJ, Choi BS, Jung C, Yoon YH, Sunwoo L, Bae HJ, et al. Differentiation of deep subcortical infarction using high-resolution vessel wall MR imaging of middle cerebral artery. *Korean J Radiol* 2017;18:964-972
21. Shaaban AM, Duerinckx AJ. Wall shear stress and early atherosclerosis: a review. *AJR Am J Roentgenol* 2000;174:1657-1665
22. Gibson CM, Diaz L, Kandarpa K, Sacks FM, Pasternak RC, Sandor T, et al. Relation of vessel wall shear stress to atherosclerosis progression in human coronary arteries. *Arterioscler Thromb* 1993;13:310-315
23. Wang Y, Qiu J, Luo S, Xie X, Zheng Y, Zhang K, et al. High shear stress induces atherosclerotic vulnerable plaque formation through angiogenesis. *Regen Biomater* 2016;3:257-267
24. Zhao ZN, Li XL, Liu JZ, Jiang ZM, Wang AH. Features of branch occlusive disease-type intracranial atherosclerotic stroke in young patients. *BMC Neurol* 2018;18:87
25. Kim JM, Jung KH, Sohn CH, Moon J, Han MH, Roh JK. Middle cerebral artery plaque and prediction of the infarction pattern. *Arch Neurol* 2012;69:1470-1475

https://doi.org/10.3348/kjr.2021.0615